Available online at www.sciencedirect.com
ScienceDirect
Quaternary Research 68 (2007) 151–161
QUATERNARY RESEARCH
www.elsevier.com/locate/yqres

Timing of surficial process changes down a Mojave Desert piedmont

Kyle K. Nichols [a,*], Paul R. Bierman [b], Martha C. Eppes [c], Marc Caffee [d,1], Robert Finkel [d], Jennifer Larsen [e]

[a] Department of Geosciences, Skidmore College, 815 N. Broadway, Saratoga Springs, NY 12866, USA
[b] School of Natural Resources and Department of Geology, University of Vermont, Burlington, VT 05405, USA
[c] Department of Geography and Earth Science, University of North Carolina Charlotte, Charlotte, NC 28223, USA
[d] Center for Accelerator Mass Spectrometry, Lawrence Livermore National Laboratory, Livermore, CA 94405, USA
[e] Department of Geology, University of Vermont, Burlington, VT 05405, USA

Received 27 January 2006
Available online 29 March 2007

Abstract

We measured ^{10}Be and ^{26}Al in 29 sediment samples to infer the history and millennial-scale rates of change down a low-gradient piedmont, a common but enigmatic landform that dominates the Mojave Desert. Nuclide data suggest that a large volume of sediment was deposited on the proximal East Range Road piedmont in Fort Irwin, California, ~75,500 yr ago. Since then, this material has been stable or eroding slowly. In contrast, on the distal piedmont (3.5 km from the upland source basins) soil stratigraphy suggests that there have been alternating periods of surface stability, erosion, and deposition over the last 70,000 yr. Nuclide data from samples amalgamated along cross-piedmont transects suggest that long-term average down-gradient sediment speeds range from 9 cm yr^{-1} near the uplands to 22 cm yr^{-1} 6 km down-piedmont. These speeds are similar to ^{10}Be-estimated sediment speeds down three other piedmonts in the Mojave Desert, suggesting that piedmont surface morphologies dominated by shallow migrating channels have similar sediment transport rates. The timing of surface process change down the East Range Road piedmont is determined by a combination of sediment available in the source basins, sediment transport rates, and the size of the piedmont.

Keywords: Cosmogenic nuclides; Sediment transport; Arid zone; Soil; Sediment budget

Introduction

Piedmonts, low-gradient surfaces that extend away from desert uplands, are common landforms in the Mojave and other deserts (O'Hara, 1997); however, the rate and timing of surface processes including sediment deposition, sediment erosion, and sediment transport remain poorly quantified over long temporal scales. Recently, measurement of cosmogenic nuclides, and interpretation of these data using mathematical models, have allowed long-term process rates on desert piedmonts to be inferred quantitatively (Brown et al., 2003; Nichols et al., 2002, 2005a,b; Phillips et al., 1998). Such studies suggest that piedmont process rates, including average down-slope sediment speeds (tens of meters to decimeters per year), sediment deposition rates (mm per kyr), and the timing of depositional hiatuses (process transition), depend on the complexity of piedmont surface and on the timing of climate change (Nichols et al., 2005b). Only through better quantification of rates and dates of surface processes can we begin to establish trends in landscape behavior, both down-piedmont and regionally. In this paper, we use cosmogenic nuclides and soils data to constrain nuclide-based models of piedmont deposition, erosion, and surface stability and compare these data to other established process rates.

Desert piedmonts

Most understanding of desert piedmont process rates comes either from direct observation, measurement, or modeling (Abrahams et al., 1988; Cooke, 1970; Rahn, 1967). Direct measurement of piedmont processes provides data for only a few years or at most a decade or two and are thus representative

* Corresponding author. Fax: +1 518 580 5199.
E-mail address: knichols@skidmore.edu (K.K. Nichols).
[1] PRIME Laboratory, Purdue University, West Lafayette Indiana 47907, USA.

0033-5894/$ - see front matter © 2007 University of Washington. All rights reserved.
doi:10.1016/j.yqres.2007.02.001

only of the short time period over which the data were collected (Persico et al., 2005; Reid and Laronne, 1995; Schick et al., 1987); extrapolation is uncertain because measurements may not capture geomorphically significant events (Kirchner et al., 2001; Trimble, 1977). Alternatively, controlled models of simulated rainfall on desert piedmonts or in flumes (Abrahams et al., 1988) can replicate changing climatic regimes. However, simulation models only quantify process rates for small, uniform areas (1 to 10 m^2). Scaling experimental results to an entire piedmont and longer time scales is uncertain.

Long-term piedmont process rates are difficult to quantify because sediment transport, deposition, and erosion are affected by changing climate and piedmont morphology (Bull, 1991; Denny, 1967). Soil development is a powerful qualitative tool for investigating the long-term behavior of piedmonts because soil genesis depends on physical and chemical parameters that can be quantified (Birkeland, 1999; McFadden et al., 1989; Wells et al., 1987). However, soil development depends on several difficult-to-measure regional variables, including carbonate and dust influx as well as microclimate (Birkeland, 1999); therefore, soil data provide at best semi-quantitative or relative piedmont histories. In the Mojave Desert region most age constraint is provided by radiocarbon and correlation of soil development (Harvey and Wells, 2003; McDonald et al., 2003).

Studying piedmont morphology allows one to define qualitatively the dominant processes modifying the surface. *Simple* planar piedmonts have one active surface, all of which is essentially one age, modern. Such simple piedmonts may experience sheetfloods, where all exposed sediment is transported down-piedmont (McGee, 1897; Rahn, 1967) or simple piedmonts may have shallow ephemeral channels that migrate laterally over the entire piedmont surface on sub-millennial time scales (Nichols et al., 2002). In contrast, *complex* piedmonts (piedmonts with multiple geomorphic surfaces of varying ages) have sediment that is usually transported in discrete and incised ephemeral channels over only a small percentage of the surface area (Bull, 1991; Denny, 1967). On complex piedmonts, sediment erosion, deposition, and transport may occur all at the same time in different places (Bull, 1991; Denny, 1967; Nichols et al., 2005b).

Geologic setting

The National Training Center (2600 km^2) at Fort Irwin in the northern Mojave Desert in southeastern California, contains numerous desert piedmonts. We studied the East Range Road piedmont (18 km^2) because the upland source is quartz-rich, ideal for ^{10}Be analysis, and because the piedmont extends several kilometers from the rangefront (Fig. 1). The uplands that supply sediment to the East Range Road piedmont consist of poorly indurated Tertiary alluvial fan deposits (clay to boulders mostly derived from granitic parent material) and have a maximum relief of ~300 m.

The East Range Road piedmont is divided into two sections, proximal and distal. The proximal piedmont extends ~1.5 km down-piedmont. This portion of the piedmont contains higher surfaces (incised <4 m by ephemeral channels) that exhibit weak desert pavement and some varnish (Fig. 2A). Clasts of soil carbonate at some surface locations suggest that the proximal piedmont was stable and is now eroding. Beyond ~1.5 km from the mountain front, the incised surfaces and the ephemeral channels merge to form a broad active surface, the distal piedmont (Fig. 2B). The active, distal surface is not incised and it lacks large clasts, pavement, and varnish, and thus it appears that all sediment has recently been transported. The average slope from the uplands to 6 km away, where the piedmont diffuses into an ephemeral trunk drainage, is a very flat 1.9°.

The climate of the East Range Road piedmont is warm and dry. At Barstow, California, ~60 km south of East Range Road, average maximum temperature ranges from 15.4 °C in December to 39 °C in July and an average of 10.3 cm of rain falls annually (EarthInfo, 2001). Most of the precipitation

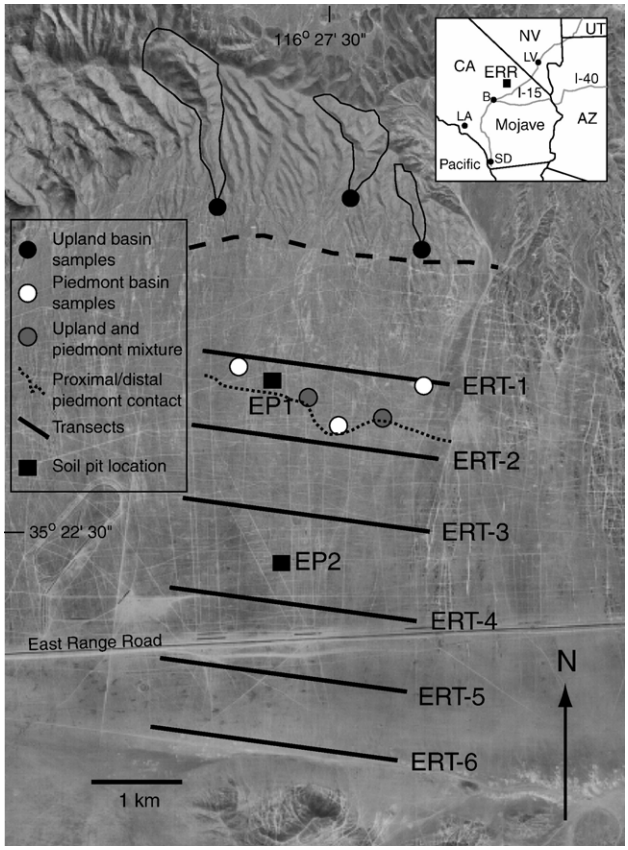

Figure 1. Aerial photograph of the East Range Road piedmont. Upland/piedmont contact represented by thick dashed line. Upland basin sample (ERV-UB) is amalgamation of sediment collected from three locations. Source basins are outlined by thin black lines. Thick black lines spaced at 1-km intervals represented transect locations (3 km long; ERT designation) from which 21 samples spaced 150 m apart were amalgamated. Black boxes represent soil pit locations (EP1 and EP2). The eroding proximal piedmont sample (ERV-P) is an amalgamation of sediment collected from channels draining only the incised alluvial surface. The sample that contains sediment sourced from both the source basins and the eroding piedmont (ERV-LB) was amalgamated from samples collected at sites marked by two gray dots. Approximate proximal/distal piedmont contact is represented by dotted black line. Faint white lines on piedmonts are roads used by tanks and wheeled vehicles. Inset map shows location of East Range Road (ERR) in the Mojave Desert. CA=California, NV=Nevada, UT=Utah, AZ=Arizona, LA=Los Angeles, LV=Las Vegas, SD=San Diego, B=Barstow, I-40=Interstate 40 and I-15=Interstate 15.

https://doi.org/10.1016/j.yqres.2007.02.001 Published online by Cambridge University Press

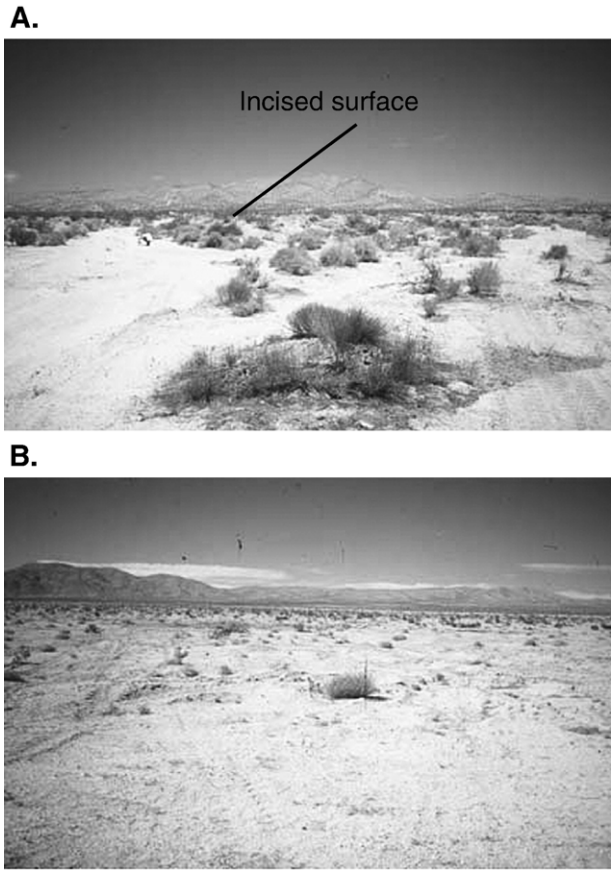

Figure 2. Photographs of the East Range Road piedmont surface. (A) Proximal piedmont surface incised approximately 1.5 m. (B) Photograph of distal wash surface on the East Range Road piedmont near ERT-4 (Fig. 1). Off-road vehicle use has destroyed the piedmont drainage network and most vegetation.

comes either in short-duration intense summer cyclonic events or in long-duration, less intense winter frontal storms.

Methods

In order to quantify rates of sediment generation and transport and to determine the piedmont's surface history, we collected sediment samples from 3 different types of basin morphology, 2 soil pits, and 5 transects. The basin samples included sediment sourced only from the uplands (ERV-UB), sediment sourced only from the eroding proximal piedmont (ERV-P), and sediment that results from a mixture of upland and piedmont sediment (ERV-LB; Fig. 3). The soil pits were located on the proximal and distal piedmont surface and transect samples were spaced at 1-km intervals down the piedmont.

Basin samples

The upland source basins provide the baseline nuclide concentration of sediment entering the piedmont (Fig. 1). These samples were used to determine source basin sediment generation rates (Bierman and Steig, 1996; Brown et al., 1995; Granger et al., 1996) and thus the long-term flux of sediment onto the piedmont. In order to determine both the mass and cosmogenic nuclide contribution of the proximal piedmont surface, we amalgamated sediment from three active ephemeral drainages that incise the proximal piedmont.

The sediment supplied to the distal piedmont is a mixture of sediment derived from the uplands (ERV-UB; Fig. 3) and sediment derived from erosion of the incised proximal piedmont surface (ERV-P; Fig. 3). We collected a sediment sample at the end of the proximal piedmont from the channels that originate in the uplands, but also are fed by smaller channels arising on the proximal piedmont (ERV-LB). Since upland- and proximal piedmont-derived sediments have different nuclide activities, a simple two component-mixing model, based on the percentage of nuclides contributed by ERV-UB and ERV-P to equal the nuclide activity of ERV-LB, determines the percentage of sediment entering the piedmont from each source.

Soil pit samples

Two pits (2.0 m and 1.4 m deep) were excavated to quantify past piedmont processes of deposition, erosion, and soil formation (Fig. 1). One pit (EP1) was located on the proximal piedmont, close to the uplands (1.5 km); the other (EP2) was located on the distal piedmont surface ~3.5 km from the uplands. Based on soil stratigraphy and horizonation, we divided each pit into contiguous depth intervals, so that samples from the entire pit walls were collected for analysis (Table 1).

Transect samples

We collected sediment along five 3-km-long transects spaced at 1-km intervals down the East Range Road piedmont to quantify the cosmic-ray dosing of sediment transported down the distal piedmont surface (ERT-2 to ERT-6; Fig. 1). Each transect sample consisted of mixing ~100 cm^3 of surface

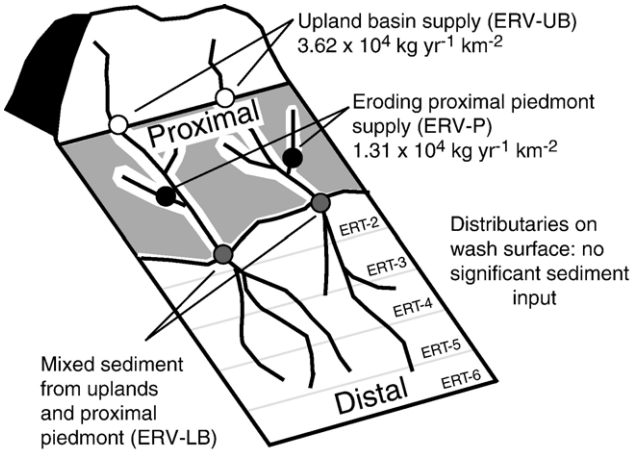

Figure 3. Schematic sediment budget for East Range Road piedmont. Uplands (ERV-UB) supply 75% of sediment to distal piedmont (white) while the eroding proximal piedmont (shaded gray; ERV-P) supplies 25%. The percentage of upland- and proximal piedmont-sourced sediment is calculated from the average nuclide concentration of the mixed sediment entering the distal piedmont (EV-LB).

https://doi.org/10.1016/j.yqres.2007.02.001 Published online by Cambridge University Press

Table 1
Soil pit descriptions for the East Range Road piedmont

Pit	Horizon [a]	Depth (cm)	Color [b]		Texture [c]	Structure [d]	Carbonate [e]
			Moist	Dry (%)			
EP1	Av	0–6	10YR 4/4	10YR 6/3	L	3 c pl	
	Bwk	6–16	7.5YR 4/4	10YR 5/4	L	f/m sbk	ef
	Bt	16–44	7.5YR 4/6	7.5YR 5/4	SL	2 m/c sbk	
	Btk	44–59	7.5YR 5/6	7.5YR 5/4	L	2 f/m sbk	stage II
	Btk_2	59–77	7.5YR 4/4	7.5YR 5/4	SL	1 f sbk	stage I
	Ck	77–100	7.5YR 4/4	10YR 6/4	LS	0.5 vf sbk	ef
	2Ck/K	100–200					
	Ck_2		10YR 4/4	10YR 6/3	LS	sg	
	K		10YR 5/4	10YR 7/3	LS	m	stage III
EP2	A	0–5	10YR 4/3	10YR 6/4	LS	sg	
	Av	5–11	10YR 4/3	10YR 6/4	LS	2 m sbk	
	Bw	11–29	10YR 4/4	10YR 6/3	LS	2 m/c sbk	
	Ck	29–43	10YR 4/4	10YR 6/4	LS	1 f sbk	ef
	2Bkmb	43–60	7.5YR 5/4	10YR 6/5	LS	2 vf sbk	ef
	2Ckb	60–84	10YR 5/4	10YR 6/5	LS	1 f sbk	ef
	$2Btbk_2$	84–106	10YR 5/4	10YR 6/5	LS	2 m sbk	ef
	$3Ck_2$	106–118	10YR 5/4	10YR 6/4	LS	1 vf sbk	ef
	$3Kb_3$	118–140	10YR 5/4	10YR 7/3	LS	m	stage III

[a] Numbers preceding the horizon designation represent the following: for EP1 1=gravelly sand, 2=sandy gravel; for EP2 overall coarsening-down sequence from 1 to 3.
[b] Color determined using Munsel color charts.
[c] Textures are defined as L=loam, SL=sandy loam, and LS=loamy sand.
[d] Structure defined as c=coarse, pl=platy, f=fine, m=medium, sbk=sub-angular blocky, vf=very fine, sg=sand and gravel.
[e] Carbonate development defined as ef=effervesces with dilute HCl.

sediment (top 10 cm) collected from 21 sampling locations equally spaced at 150-m intervals (piedmont transects).

Sediment that is in active transport, termed the *active transport layer (ATL)*, is usually determined from the thickness of well-mixed sediment above the top of the maximally developed and often truncated B-horizon (Lekach et al., 1998; Nichols et al., 2002). In shallow soil pits excavated to the buried B-horizon on the distal portion of the East Range Road piedmont, the depth to the buried B-horizon decreased from 30 cm at ERT-2 to 10 cm at ERT-6, not significantly different than the decimeter-scale thickness of several other Mojave Desert piedmonts (Nichols et al., 2002, 2005b).

Laboratory methods

All samples were processed using accepted methods (Bierman and Caffee, 2001; Kohl and Nishiizumi, 1992). We analyzed quartz in the 500- to 850-μm size (coarse sand) fraction to minimize the possibility of analyzing eolian sediment (fine sand to coarse silt). Because different grain sizes in arid regions have statistically similar nuclide activities (Clapp et al., 2000, 2001, 2002; Granger et al., 1996) we did not analyze other grain size fractions. Accelerator mass spectrometry (AMS) analysis, at Lawrence Livermore National Laboratory, determined blank-corrected $^{10}Be/^{9}Be$ and $^{26}Al/^{27}Al$ ratios. We interpreted the nuclide data using nominal production rates (sea level and >60° latitude) of 5.2 ^{10}Be atoms g^{-1} yr^{-1} and 30.4 ^{26}Al atoms g^{-1} yr^{-1} (Bierman et al., 1996; Gosse and Phillips, 2001; Stone, 2000) scaled for altitude and latitude using no muons (Lal, 1991).

Interpretive models

We used previously published models of nuclide activity in sediment to estimate long-term basin erosion and sediment generation rates (Brown et al., 1995; Clapp et al., 2000, 2002; Granger et al., 1996), to quantify surface stability (Anderson et al., 1996), to quantify deposition rates (Lal and Arnold, 1985; Nichols et al., 2005b; Phillips et al., 1998), and to determine the duration of depositional hiatuses (Nichols et al., 2005b). Sediment transport models used a nuclide-balance approach to translate nuclide concentrations measured in piedmont sediment into long-term average sediment transport velocities (Nichols et al., 2002). East Range Road piedmont surface processes operate on time scales much shorter than the nuclide half-lives (^{10}Be=1.5 Myr, ^{26}Al=0.7 Myr); therefore, surface processes control nuclide activities, not radioactive decay. Since the uplands are dominantly quartz-rich Tertiary fan deposits, we assumed no quartz enrichment through preferential dissolution of other minerals at East Range Road (Small et al., 1999).

Results

The ^{10}Be and ^{26}Al data are consistent with simple exposure histories without extended periods of burial during or after dosing; measured ratios ($^{26}Al/^{10}Be$) do not diverge significantly from the production ratio of 6.0 (Table 2; Fig. 4; Nishiizumi et al., 1989). Measurement precision averages 3% for ^{10}Be and 5% for ^{26}Al; therefore, we base our models on ^{10}Be data because they are more precisely measured.

https://doi.org/10.1016/j.yqres.2007.02.001 Published online by Cambridge University Press

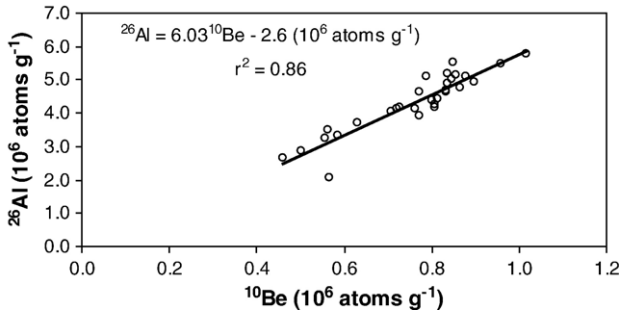

Figure 4. Regression of the ^{10}Be and the ^{26}Al data. The regression trendline of entire data set has a slope similar to the nominal production ^{10}Be/^{26}Al ratio of 6.0 (Nishiizumi et al., 1989) indicating no significant burial during or after exposure and no significant nuclide inheritance from Tertiary source basin rocks.

Basin results

The upland basin samples have the lowest average nuclide activity ($0.459 \pm 0.015 \times 10^6$ ^{10}Be atoms g^{-1}; ERV-UB in Fig. 5) and thus the shortest near-surface exposure history. The basins that drain only the eroding proximal section of the piedmont have higher average nuclide activities ($0.630 \pm 0.017 \times 10^6$ ^{10}Be atoms g^{-1}; ERV-P in Fig. 5), and have been more heavily dosed by cosmic radiation than upland basin sediment, a finding consistent with the time required to form pavement, varnish, and the clasts of soil carbonate now found at the surface of some locations on the proximal piedmont. The sample amalgamated from drainages crossing the eroding proximal piedmont has an intermediate nuclide activity ($0.502 \pm 0.015 \times 10^5$ ^{10}Be atoms g^{-1}; ERV-LB in Fig. 5), consistent with more-dosed sediment eroding from the proximal piedmont mixing with less-dosed sediment from the uplands.

Soil pit results

Soil development in pits EP1 and EP2 suggest that different processes modify the piedmont surface at these locations (Figs. 6 and 7). At EP1 (~1.5 km down-gradient from the uplands), soil horizonation is consistent with continual soil genesis and no distinct depositional or erosional events. From the surface to 16 cm, there is an Av and Bwk horizon, and from 16 to 77 cm there are well-developed Bt/Btk/Btk$_2$ horizons (Table 1). The bottom of the soil column has an interlayered 2Ck$_2$ and K horizon with stage III carbonate development, 100 to 200 cm, overlain by a Ck horizon, 77 to 100 cm. Soils in pit EP2 suggest a different history. Pit EP2 has three buried and truncated soils at 43, 84, and 118 cm depths. The uppermost 43 cm has weak soil development and is consistent with late-Holocene deposition. The bottom-most soil is a massive K-horizon with stage III development. Thus, the soils in EP2 are consistent with several periods of stability or erosion followed by renewed deposition.

Nuclide depth profiles for the two soil pits on the East Range Road piedmont have distinctively different shapes. Pit EP1 has nuclide concentrations that generally decrease with depth (Fig. 6). Pit EP2 has nuclide activities that neither increase nor decrease at depth (Fig. 7). The top-most three samples from pit EP1 have nuclide activities that are statistically equal to or

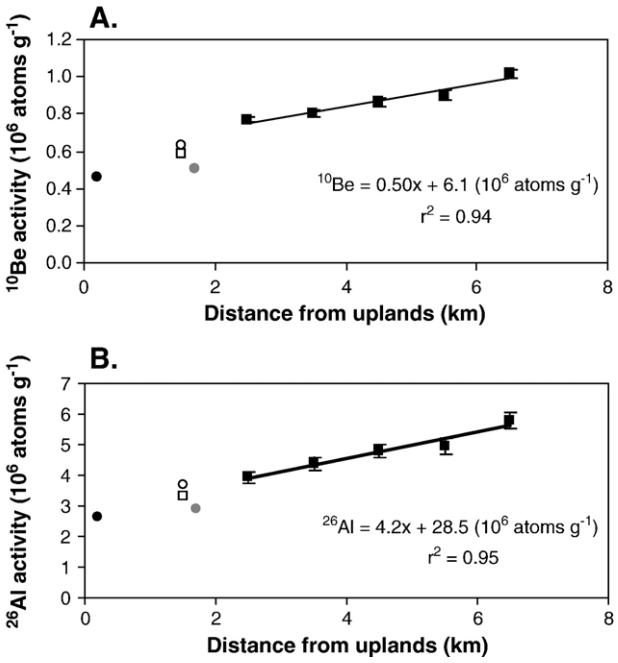

Figure 5. Nuclide activity increases down-piedmont for ^{10}Be (A) and ^{26}Al (B). Solid black squares represent transect data on wash surface (ERT 2–6). Open square represents amalgamated transect sample characterizing proximal piedmont surface sediment and ephemeral channel sediment (ERT-1). Open circle represents upland source basin sediment datum (ERV-UB). Gray circle represents eroding proximal piedmont datum (ERV-P). Black circle represents sediment mixture of ephemeral channel sediment and sediment eroded from piedmont (ERV-LB). Uncertainty is 1σ expressed by error bars, which are commonly smaller than symbol and thus not visible.

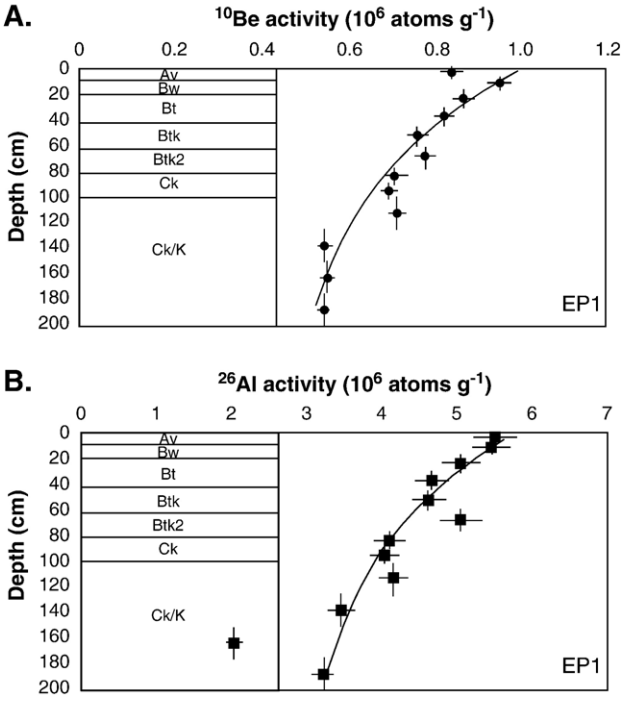

Figure 6. ^{10}Be data (A) and ^{26}Al data (B) for pit EP1. Data points represent midpoint of depth interval. Vertical error bars represent sample depth interval. Horizontal error bars represent 1σ analytical uncertainty. Black lines show model fit of 75,500 yr of surface stability. Soil data explained further in Table 1.

https://doi.org/10.1016/j.yqres.2007.02.001 Published online by Cambridge University Press

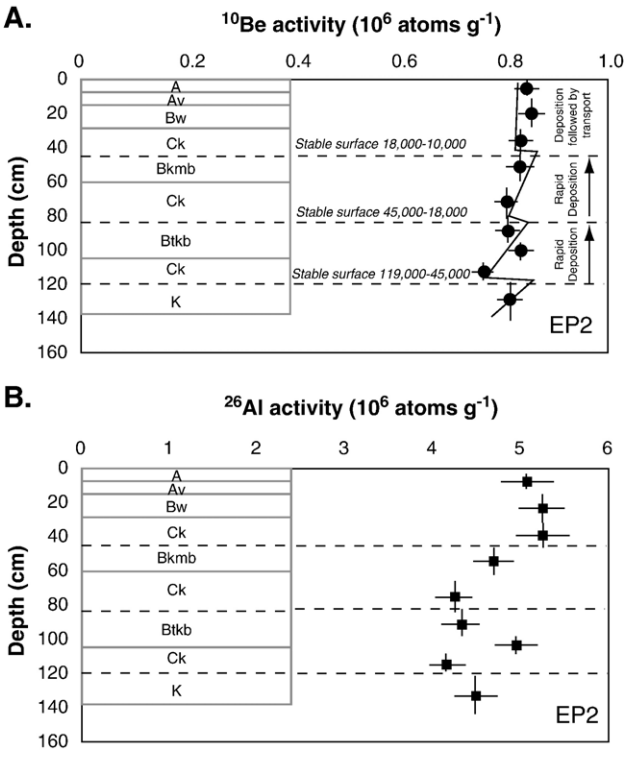

Figure 7. ^{10}Be data (A) and ^{26}Al data (B) for pit EP2. Nuclide activity neither increases nor decreases systematically with depth. Data points represent midpoint of depth interval. Vertical error bars represent sample depth interval. Horizontal error bars represent 1σ analytical uncertainty. Black line shows model fit explained in text. Dashed lines represent buried soil horizons. Number range represents period of stability in years before present. Soil data explained further in Table 1.

greater than all samples from EP2 (Table 2). This indicates that sediment on the stable proximal piedmont surface has higher concentrations of ^{10}Be and ^{26}Al than sediment on the mobile distal piedmont.

Transect results

Nuclide activities for the piedmont transects increase in a nearly linear fashion from $0.771 \pm 0.021 \times 10^6$ ^{10}Be atoms g^{-1} at ERT-2 at the proximal/distal transition to $1.02 \pm 0.04 \times 10^6$ ^{10}Be atoms g^{-1} at ERT-6, the most distal transect (Fig. 5). The nuclide activity at the beginning of the distal piedmont (ERT-2) is a mixture of upland basin sediment ($0.459 \pm 0.015 \times 10^6$ ^{10}Be atoms g^{-1}), sediment derived from the surface of the proximal piedmont (ERV-P; $0.630 \pm 0.017 \times 10^6$ ^{10}Be atoms g^{-1}), and sediment input from bank incision and collapse (represented by the depth-weighted average of samples from soil pit EP1, 0.555 ± 0.016 to $0.959 \pm 0.028 \times 10^6$ ^{10}Be atoms g^{-1}). The increase of nuclide activity down-piedmont reflects the continued dosing of sediment during transport.

Discussion

Nuclide data provide insight into the long-term behavior of the East Range Road piedmont. Field observations indicate that sediment is generated from the uplands and from the eroding proximal piedmont. The upland source basins are lowering at a rate (average of ^{10}Be and ^{26}Al data) of 13 ± 3 mm kyr^{-1}. This rate is low compared to other basin-wide erosion rates in the arid southwest (Clapp et al., 2001, 2002; Granger et al., 1996; Nichols et al., 2002, 2005a). Perhaps low sediment-generation rates in the East Range Road uplands reflect greater infiltration capacity and low runoff yield of the indurated Tertiary alluvial fan deposits, and thus possibly different slope processes, compared to bare slopes of crystalline bedrock feeding sediment to other piedmonts studied using cosmogenic nuclides. The eroding proximal piedmont supplies additional sediment to the distal piedmont surface. Using the two-component mixing-model, 75% of the nuclide contribution of ERV-LB is sourced from the uplands while 25% of the nuclide contribution is from the proximal piedmont. Therefore, the upland source basins supply 75% of sediment (3.62×10^4 kg yr^{-1} km^{-2}) to the distal piedmont while the more highly dosed, incised proximal piedmont supplies 25% of the sediment (1.31×10^4 kg yr^{-1} km^{-2}; Fig. 3).

Soil pit interpretive models

Proximal piedmont pit (EP1)

Nuclide activity in the soil pit located on the proximal incised alluvial surface (EP1) decreases as a function of depth, suggesting rapid sediment deposition followed by a significant period of stability (Phillips et al., 1998). Using Monte Carlo simulation and averaging the ^{10}Be and ^{26}Al results suggests that the proximal piedmont surface is at least 75,500 yr old (Fig. 6; Anderson et al., 1996). Using the approach of Anderson et al. (1996), the calculated nuclide activity at the time of deposition for sediment exposed today in pit EP1 was 4.5×10^5 atoms g^{-1}, similar to the nuclide activity of sediment currently issuing from the upland basins ($4.6 \pm 0.1 \times 10^5$ atoms g^{-1}). Such consistency in nuclide activity suggests that the contemporary average source basin erosion rates are similar to the average source basin erosion rates of 75,500 yr ago. The ≥75,500-yr age of the eroding piedmont is consistent with the degree of soil development in the pit and the K-horizon (stage III carbonate) at the bottom of the pit (Birkeland, 1999).

Distal piedmont pit (EP2)

Three distinct buried soil horizons, exposed in pit EP2 at depths of 43 cm, 84 cm, and 118 cm, represent periods of surface stability on the distal piedmont; however, nuclide activities neither increase nor decrease with depth in this pit as would be expected from dosing during extended periods of soil formation (Phillips et al., 1998) (Fig. 7). Reconciling nuclide and soils data requires that the initial nuclide activities of the sediment deposited at the soil pit location changed over time. Such changes could reflect differing mixtures of upland source basin sediment and sediment eroded from the proximal piedmont or upslope portions of the distal piedmont. Using a mathematical model of nuclide accumulation in aggrading soils (Nichols et al., 2002) and Monte Carlo simulation about a normal distribution of the nuclide mean concentration values,

https://doi.org/10.1016/j.yqres.2007.02.001 Published online by Cambridge University Press

we create a plausible scenario of alternating periods of deposition and stability/erosion on the distal piedmont (EP2) that incorporates increasing nuclide inheritance over time. The nuclide activities range from a low determined by the sediment that is currently issuing from the uplands ($4.6 \pm 0.15 \times 10^5$ atoms g^{-1}) to a high represented by the nuclide activity of the sediment located 3.5 km from the uplands ($8.5 \pm 0.25 \times 10^5$ atoms g^{-1}).

Such modeling suggests the timing and duration of stability associated with each buried soil and depositional period. The horizonation of each buried soil suggests some amount of soil erosion before the subsequent depositional period. If we assume erosion of 1 m of soil from above the $3Kb_3$ horizon, the surface was stable for about 74,000±11,000 yr from 119,000 to 45,000 yr ago. At 45,000 yr ago, a pulse of sediment with higher nuclide inheritance, buried the $3Kb_3$ horizon. The presence of a $2Btbk_2$ horizon suggests a thinner stripping of soil than the $3Kb_3$ horizon. Assuming 20 cm of soil stripping, the $2Btbk_2$ is associated with about 27,000±3,000 yr of stability to about 18,000 yr ago. At 18,000 yr ago a pulse of deposition, with higher nuclide inheritance, buried the $2Btbk_2$ horizon. The development of 2Bkmb horizon is also consistent with a thin layer (20 cm) of soil erosion and a model estimate of 8,000± 3,000 yr of stability. Thus, at ~10,000 yr ago the 2Bkmb horizon was buried by the topmost 43 cm of sediment. The average nuclide activity of the topmost 43 cm ($8.46 \pm 0.25 \times 10^5$ atoms g^{-1}; Fig. 7) is similar to the average nuclide activity of sediment in transport down the piedmont (8.33×10^5 atoms g^{-1}; Fig. 5) at the location (~3.5 km) of the soil pit. Since nuclide activities of sediment in transport and of sediment in the uppermost strata of the soil pit are similar, the sediment is transported on time scales of <3000 yr at this location, based on the analytical error divided by the average site-specific production rate for 20 cm of depth. Furthermore, since the uppermost 43 cm of sediment has weak soil development (Bw), this sediment has likely been in active transport down the piedmont since the end of the last period of stability 10,000 yr ago. The total time represented by these scenarios is about 120,000 yr, sufficient to develop the observed soils (Fig. 7).

Sediment transport speed

The rate of sediment movement down-piedmont can be responsible for a lag time between a change in geomorphic process in the uplands and the resulting process change on piedmonts. Piedmonts that have short travel distances or fast sediment transport speeds will adjust to changes in basin processes resulting from climate change or tectonic activity sooner than piedmonts that are longer or have slower sediment transport speeds. In order to determine the relative lag time on the East Range Road piedmont, we quantify average down-piedmont sediment speeds using a nuclide balance model (Nichols et al., 2002) based on the site-specific ^{10}Be production rate (8.63 atoms g^{-1}), soil density (1.6 g cm^{-3}), nuclide attenuation length (165 g cm^{-2}), active transport-layer thickness decreasing from 27 cm at the start of the distal piedmont to 9 cm at the distal piedmont, and ^{10}Be activity of substrate based on soil pit data (8.4×10^5 atoms g^{-1}). The model fits the data well and suggests that the average grain speed slightly increases down the East Range Road piedmont (due to a decreasing active layer depth) from 9 cm yr^{-1} at the start of the distal piedmont to 22 cm yr^{-1} at the last transect, 5 km down-gradient (Fig. 8). The total transit time of sediment moving down the East Range Road piedmont from the source basins to the last transect is thus estimated to be 62,000 yr. This long transit time represents integrated sediment transport speeds and not the instantaneous speeds during prior piedmont histories.

The integrated long-term average sediment velocities down the East Range Road piedmont are slower than but similar to the distal Chemehuevi Mountain piedmont (Nichols et al., 2005a), and the Iron and Granite Mountain piedmonts (Nichols et al., 2002; Fig. 9). On all four surfaces, nuclide activity increases regularly down-gradient and sediment speeds on active surfaces average decimeters per year. These results suggest that measurements of long-term sediment speeds are robust and similar in spite of different geologic histories.

Comparison of East Range Road piedmont to regional climate records

Our data quantify the rates and dates of surficial processes that modified the East Range Road piedmont over the last 10^4 yr. The interpretive models are constrained by age estimates provided by traditional soil analyses. Although the cosmogenic data are not as precise as a detailed radiocarbon chronology, they do allow for a regional comparison to previous work, while extending a quantitative piedmont chronology farther back into the Pleistocene than radiocarbon would allow.

Cosmogenic analysis suggests that >75,500 yr ago, a large volume of sediment was delivered to the proximal East Range Road piedmont (EP1). Other >70,000, yr depositional events in the Mojave Desert are common (Gosse et al., 2004) and are recorded in Soda Mountain alluvial fan units (Harvey and Wells, 2003), the Providence Mountains alluvial fans (McDonald and McFadden, 1994), and soils capped by basalt flows at Cima (Wells et al., 1995). The depositional event above the 118-cm-deep buried soil in the distal wash surface (EP2) about 45,000 yr ago is not time-correlative with other pulses of deposition in the Mojave Desert (Fig. 10). The

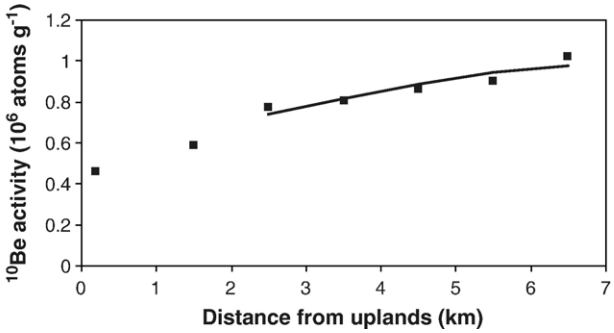

Figure 8. Best fit of nuclide mixing model (black line) to the ^{10}Be data (squares). We used the model described in Nichols et al. (2002). 1σ analytical error bars are smaller than the symbols. RMS error of the model is 33,000 atoms per gram.

https://doi.org/10.1016/j.yqres.2007.02.001 Published online by Cambridge University Press

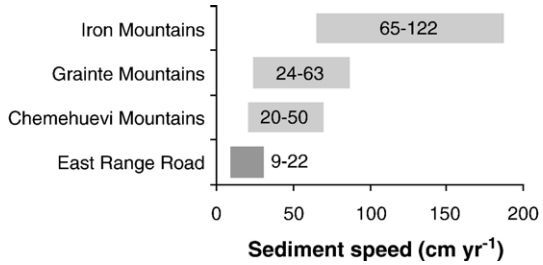

Figure 9. Cosmogenic nuclide-based sediment speeds for four piedmonts located in the Mojave Desert. Bars represent range of speed. Iron and Granite Mountain data are from Nichols et al. (2002) and the Chemehuevi Mountain data are from Nichols et al. (2005b).

timing of geomorphic change recorded in soil pit EP2 and, indeed, on many piedmonts, especially those of any substantial size, should lag hillslope response by millennia because a wave of sediment must move down-piedmont from the locus of erosion.

If we assume that the integrated sediment transport rates are representative of past rates, then ~30,000 yr would be required for changes in hillslope processes to affect the piedmont at the location of EP2, ~3.5 km from the uplands. Such a lag is consistent with the pulse of deposition about 75,000 yr ago that is clearly recorded on the proximal piedmont, followed by 30,000 yr of transgression down the piedmont, and deposition ~45,000 yr ago. Similarly, the sediment pulse at ~18,000 yr ago occurred when there were only small amounts of alluvial fan activity in the Providence Mountains (McDonald et al., 2003) and possibly the Soda Mountains (Harvey and Wells, 2003). At this time, the glacial maximum, the Mojave Desert was relatively moist; there were more frequent flooding events in the nearby Mojave River (Enzel et al., 2003; Wells et al., 2003) but sediment deposition was at a minimum (Reheis et al., 1996). Following the argument above, the 18,000 event at EP2 may reflect changes in source basin conditions closer to 50,000 yr ago or perhaps incision of the proximal piedmont and the transfer of sediment down slope, a finding consistent with model fits suggesting increasing nuclide inheritance over time in soil pit EP-2 sediments.

Several conceptual geomorphic models consider how and when surface processes in confined dryland drainage basins change in response to climate fluctuations (Bull, 1991; Harvey and Wells, 1994; McDonald et al., 2003). The prevailing theory of basin response to climate change suggests that hillslopes become transport-limited in moister climates, due to soil development, high infiltration rates, and vegetation cover. Slopes become weathering limited and sediment more mobile as vegetation disappears when climate dries (Bull, 1991). However, these models do not relate directly to the timing of process

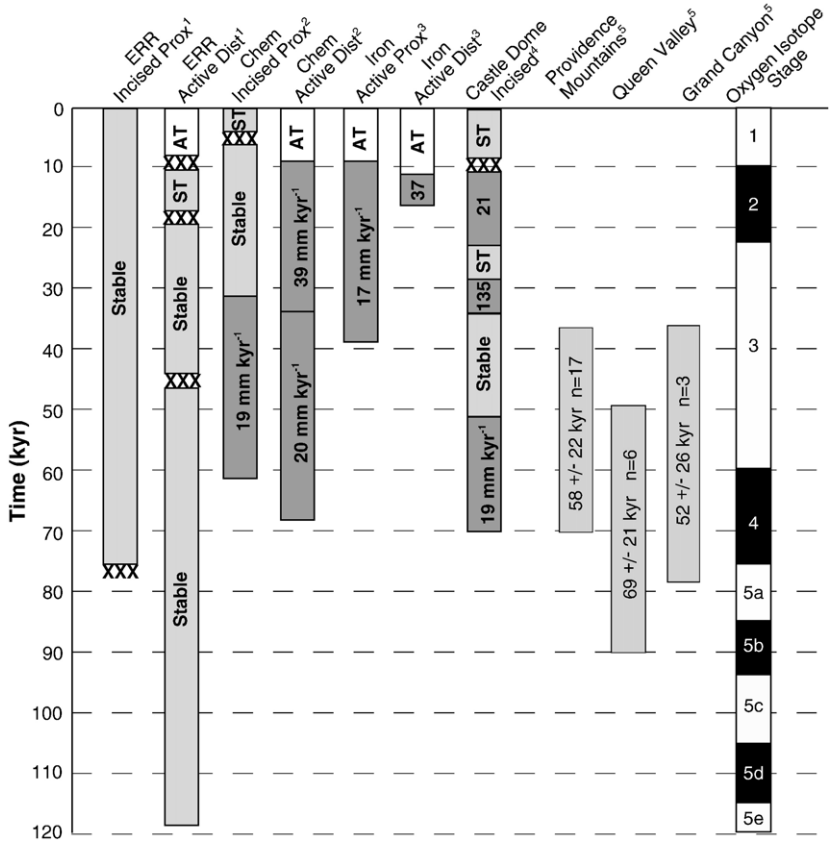

Figure 10. Comparison of piedmont processes and histories in the Mojave Desert. Dark grey boxes represent slow deposition (rates in mm kyr^{-1}), light grey boxes represent surface stability (ST), white boxes represent active transport across the surface (AT), and XXX represents a rapid pulse of deposition. Data from Providence Mountains, Queen Valley, and Grand Canyon are cosmogenic surface exposure ages (Gosse et al., 2004). Oxygen Marine Isotope stages are shown in black and white. Prox=proximal piedmont, Dist=distal piedmont, Chem=Chemehuevi Mountains.

https://doi.org/10.1016/j.yqres.2007.02.001 Published online by Cambridge University Press

Table 2
Cosmogenic nuclide data for East Range Road piedmont

Sample [a]	Elevation [b] (m)	Northing [c] (UTM)	Easting [c] (UTM)	^{10}Be activity [d] (10^6 atoms g^{-1})	^{26}Al activity [d] (10^6 atoms g^{-1})	^{26}Al/^{10}Be
ERV-UB	990	3,918,672	548,155	0.459±0.015	2.62±0.146	5.78±0.37
	1000	3,918,524	549,577			
	930	3,917,713	550,513			
ERV-LB	900	3,917,584	548,022	0.502±0.015	2.88±0.136	5.73±0.32
	840	3,916,421	549,596			
	830	3,916,107	550,302			
ERV-P	860	3,916,800	548,269	0.630±0.017	3.69±0.172	5.86±0.31
	830	3,916,069	549,922			
	860	3,916,746	550,367			
ERT-1	870	3,917,000	547,800	0.587±0.016	3.34±0.155	5.68±0.31
		3,916,750	550,800			
ERT-2	810	3,616,000	547,650	0.771±0.021	3.93±0.186	5.10±0.28
		3,915,750	550,650			
ERT-3	760	3,915,000	547,500	0.802±0.021	4.38±0.204	5.47±0.29
		3,914,750	550,500			
ERT-4	720	3,914,000	547,350	0.864±0.028	4.78±0.229	5.53±0. 32
		3,913,750	550,350			
ERT-5	695	3,913,000	547,200	0.899±0.024	4.95±0.241	5.50±0.30
		9,312,750	550,200			
ERT-6	680	3,912,200	547,050	1.018±0.035	5.78±0.269	5.68±0.33
		3,911,950	550,050			
EP1 0–6	840	3,916,585	548,869	0.850±0.026	5.54±0.289	6.51±0.39
EP1 6–16				0.959±0.028	5.49±0.256	5.73±0.31
EP1 16–30				0.877±0.025	5.08±0.256	5.79±0.34
EP1 30–44				0.833±0.022	4.69±0.227	5.64±0.31
EP1 44–59				0.773±0.023	4.66±0.217	6.03±0.33
EP1 59–77				0.790±0.023	5.08±0.272	6.44±0.39
EP1 77–90				0.719±0.027	4.14±0.202	5.75±0.36
EP1 90–100				0.707±0.018	4.07±0.185	5.75±0.30
EP1 100–125				0.726±0.019	4.18±0.190	5.76±0.30
EP1 152–150				0.562±0.016	3.49±0.172	6.21±0.35
EP1 150–175				0.566±0.016	2.07±0.102	3.65±0.21
EP1 175–200				0.555±0.016	3.25±0.152	5.86±0.32
EP2 0–11	755	3,914,895	549,055	0.847±0.023	5.00±0.288	5.91±0.38
EP2 11–29				0.856±0.026	5.17±0.248	6.03±0.34
EP2 29–43				0.837±0.023	5.18±0.291	6.19±0.39
EP2 43–60				0.835±0.027	4.63±0.219	5.55±0.32
EP2 60–84				0.808±0.022	4.19±0.189	5.18±0.28
EP2 84–95				0.808±0.021	4.26±0.204	5.27±0.29
EP2 95–106				0.836±0.023	4.88±0.233	5.84±0.32
EP2 106–118				0.762±0.021	4.12±0.194	5.40±0.30
EP2 118–140				0.815±0.023	4.43±0.234	5.44±0.33

[a] Sample notation: ER=East Range Road, V=source basin sample, UB=upland basin, LB=mixture of upland sediment and eroding sediment, P=eroding piedmont sediment. UB, LB, and P each are an amalgamation of three samples, T=transect sample, EP1 represents proximal soil pit to the uplands, EP2 represents distal soil pit located ~4 km from uplands, numbers located after EP# represent depth intervals in centimeters.

[b] All elevations are average upland valley elevation, based on basin hypsometry, and average elevation of the 3-km-long transects.

[c] Northing and Easting values are NAD 27 zone 11S UTM datum. Coordinates are listed for all averaged valley samples. Endpoint coordinates are listed for transect samples.

[d] Error is counting statistics from AMS with 2% uncertainty for stable Be and 4% uncertainty for stable Al, combined quadratically.

changes down large, unconfined desert piedmonts. The change in the rate at which sediment is translated down large piedmonts should be tied directly to source basin sediment yield as well as hydrology (Leeder et al., 1998). On large piedmont systems, small changes in sediment supply may not be measurable far from source basins.

The low sediment generation rates, low relief, and low slopes of the East Range uplands, and the highly porous source material, the Tertiary fan deposits, likely prevent fast sediment transport speeds and large sediment pulses with widespread sediment deposition, except for the most major changes in source basin behavior. Likewise, the slow sediment transport rates at East Range Road should produce long lag times causing the timing of piedmont response to be out of phase with source basin behavior. Such long lag times in response to climate change have been suggested for major river systems such as the Rio Puerco and its headwaters (Clapp et al., 2001) and the Colorado River and its tributaries (Anders et al., 2005). Here we interpret nuclide data to suggest that large piedmonts with slow sediment transport systems are similarly out of phase with climate forcings. Denser spatial coverage of dated soil pits would be required to fully test this hypothesis; however,

https://doi.org/10.1016/j.yqres.2007.02.001 Published online by Cambridge University Press

correlation between different piedmonts cannot be made reliably until down-piedmont lag times are well constrained.

Conclusions

Cosmogenic nuclide data from the East Range Road piedmont suggest a complex history of deposition, erosion, stability, and transport over the past ~120,000 yr. Source basins, composed of Tertiary fan deposits, produce sediment at lower rates than bedrock basins in the Mojave Desert. About 75,000 yr ago, a pulse of sediment was deposited on the proximal piedmont and has been stable or slowly eroding since. It is possible that the depositional event took ~30,000 yr, based on our measured sediment speeds, to propagate 3.5 km to the distal piedmont where we identified a depositional event ~45,000 yr ago. A subsequent depositional event about 18,000 yr ago was also measured on the distal piedmont but is out of phase with other Mojave Desert depositional events. Since the Pleistocene/Holocene transition, the distal piedmont has been active, as suggested by minimal soil development and uniform nuclide activities; here, transport dominates erosion and deposition. The timing of process changes on large piedmonts depends on a combination of sediment supply, sediment transport rates, and the distance from the source basins. Using cosmogenic nuclides to quantify histories in a series of soil pits down a piedmont will allow improved understanding of both the timing and distribution of piedmont processes and thus allow more robust process and temporal linkages to changing climate.

Acknowledgments

We thank L. Persico for field assistance, R. Sparks and the ITAM crew for logistical support, A. Matmon and B. Copans for sample preparation assistance, and P. Fahnstock for excavating soil pits. E. Taylor and an anonymous reviewer provided important comments that improved this manuscript. Research supported by grant #DAAD199910143 to Bierman and the Jonathan O. Davis and J. Hoover Mackin scholarships to Nichols.

References

Abrahams, A.D., Parsons, A.J., Luk, S.H., 1988. Hydrologic and sediment responses to simulated rainfall on desert hillslopes in southern Arizona. Catena 15, 103–117.

Anders, M., Pederson, J., Rittenour, T.M., Sharp, W.D., Gosse, J.C., Karlstrom, K.E., Crossey, L.J., Goble, R.J., Stockli, L., Yang, G., 2005. Pleistocene geomorphology and geochronology of eastern Grand Canyon: linkages of landscape components during climate changes. Quaternary Science Reviews 24, 2428–2448.

Anderson, R.S., Repka, J.L., Dick, G.S., 1996. Explicit treatment of inheritance in dating depositional surfaces using in situ ^{10}Be and ^{26}Al. Geology 24, 47–51.

Bierman, P.R., Caffee, M.W., 2001. Slow rates of rock surface erosion and sediment production across the Namib Desert and escarpment, Southern Africa. American Journal of Science 301, 326–358.

Bierman, P.R., Steig, E.J., 1996. Estimating rates of denudation using cosmogenic isotope abundances in sediment. Earth Surface Processes and Landforms 21, 125–139.

Bierman, P., Larson, P., Clapp, E., Clark, D., 1996. Refining estimates of 10-Be and 26-Al production rates. Radiocarbon 38, 149.

Birkeland, P.W., 1999. Soils and Geomorphology. Oxford Univ. Press, New York.

Brown, E.T., Stallard, R.F., Larsen, M.C., Raisbeck, G.M., Yiou, F., 1995. Denudation rates determined from the accumulation of in situ-produced ^{10}Be in the Luquillo Experimental Forest, Puerto Rico. Earth and Planetary Science Letters 129, 193–202.

Brown, E.T., Colin, F., Bourles, D.L., 2003. Quantitative evaluation of soil processes using in situ-produced cosmogenic nuclides. Comptes Rendues Geoscience 335, 1161–1171.

Bull, W.B., 1991. Geomorphic Responses to Climate Change. Oxford Univ. Press, New York.

Clapp, E.M., Bierman, P.R., Schick, A.P., Lekach, J., Enzel, Y., Caffee, M., 2000. Sediment yield exceeds sediment production in arid region drainage basins. Geology 28, 995–998.

Clapp, E.M., Bierman, P.R., Nichols, K.K., Pavich, M., Caffee, M., 2001. Rates of sediment supply to arroyos from upland erosion determined using in situ-produced cosmogenic ^{10}Be and ^{26}Al. Quaternary Research 55, 235–245.

Clapp, E.M., Bierman, P.R., Caffee, M., 2002. Using ^{10}Be and ^{26}Al to determine sediment generation rates and identify sediment source areas in an arid region drainage. Geomorphology 45, 89–104.

Cooke, R.U., 1970. Morphometric analysis of pediments and associated landforms in the western Mojave Desert, California. American Journal of Science 269, 26–38.

Denny, C.S., 1967. Fans and pediments. American Journal of Science 265, 81–105.

EarthInfo, 2001. NCDC Summary of the Day data CD, Boulder.

Enzel, Y., Wells, S.G., Lancaster, N., 2003. Late Pleistocene lakes along the Mojave River, southeast California. In: Enzel, Y., Wells, S.G., Lancaster, N. (Eds.), Paleoenvironments and Paleohydrology of the Mojave and Southern Great Basin Deserts. Geological Society of America, Boulder, CO, pp. 61–77.

Gosse, J.C., Phillips, F.M., 2001. Terrestrial in situ cosmogenic nuclides: theory and application. Quaternary Science Reviews 20, 1475–1560.

Gosse, J., McDonald, E., Pederson, J., Stockli, D., Lee, J., Stockli, L., Yang, G., 2004. Oxygen isotope stage 4 sediment dominates the U.S. southwest alluvial record. Geological Society of America Abstracts with Programs 36, 307.

Granger, D.E., Kirchner, J.W., Finkel, R., 1996. Spatially averaged long-term erosion rates measured from in situ produced cosmogenic nuclides in alluvial sediment. The Journal of Geology 104, 249–257.

Harvey, A.M., Wells, S.G., 1994. Late Pleistocene and Holocene changes in hillslope sediment supply to alluvial fan systems: Zzyzx, California. In: Millington, A.C., Pye, K. (Eds.), Environmental Change in Drylands: Biogeographical and Geomorphological Perspectives. Wiley, Chichester.

Harvey, A.M., Wells, S.G., 2003. Late Quaternary variations in alluvial fan sedimentologic and geomorphic processes, Soda Lake basin, eastern Mojave Desert, California. In: Enzel, Y., Wells, S.G., Lancaster, N. (Eds.), Paleoenvironments and Paleohydrology of the Mojave and Southern Great Basin Deserts. Geological Society of America, Boulder, CO, pp. 207–230.

Kirchner, J.W., Finkel, R.C., Riebe, C.S., Granger, D.E., Clayton, J.L., King, J.G., Megahan, W.F., 2001. Mountain erosion over 10 yr, 10 k.y., and 10 m.y. time scales. Geology 29, 591–594.

Kohl, C.P., Nishiizumi, K., 1992. Chemical isolation of quartz for measurement of in situ-produced cosmogenic nuclides. Geochimica et Cosmochimica Acta 56, 3583–3587.

Lal, D., 1991. Cosmic ray labeling of erosion surfaces: in situ nuclide production rates and erosion models. Earth and Planetary Science Letters 104, 424–439.

Lal, D., Arnold, J.R., 1985. Tracing quartz through the environment. Proceeding of the Indian Academy of Science 94, 1–5.

Leeder, M.R., Harris, T., Kirby, M., 1998. Sediment supply and climate change: implications for basin stratigraphy. Basin Research 10, 7–18.

Lekach, J., Amit, R., Grodek, T., Schick, A.P., 1998. Fluvio-pedogenic processes in an ephemeral stream channel, Nahal Yael, Southern Negev, Israel. Geomorphology 23, 353–369.

McDonald, E.V., McFadden, L.D., 1994. Quaternary stratigraphy of the Providence Mountains piedmont and preliminary age estimates and regional

stratigraphic correlations of Quaternary deposits in the eastern Mojave Desert California. In: McGill, S.F., Ross, T.M. (Eds.), Geological Investigations of an Active Margin: Geological Society of America, Cordilleran Section Field Trip Guidebook. Geological Society of America, Boulder, CO, pp. 205–210.

McFadden, L.D., Ritter, J.B., Wells, S.G., 1989. Use of multiparameter relative-age methods for age estimation and correlation of alluvial fan surfaces on a desert piedmont, eastern Mojave Desert, California. Quaternary Research 32, 276–290.

McDonald, E.V., McFadden, L.D., Wells, S.G., 2003. Regional response of alluvial fans to the Pleistocene–Holocene climatic transition, Mojave Desert, California. In: Enzel, Y., Wells, S.G., Lancaster, N. (Eds.), Paleoenvironments and Paleohydrology of the Mojave and Southern Great Basin Deserts. Geological Society of America, Boulder, CO, pp. 189–205.

McGee, W.J., 1897. Sheetflood erosion. Bulletin of the Geological Society of America 8, 87–112.

Nichols, K.K., Bierman, P.R., Hooke, R.L., Clapp, E.M., Caffee, M., 2002. Quantifying sediment transport on desert piedmonts using ^{10}Be and ^{26}Al. Geomorphology 45, 105–125.

Nichols, K.K., Bierman, P.R., Caffee, M., Finkel, R., Larsen, J., 2005a. Cosmogenically enabled sediment budgeting. Geology 33, 133–136.

Nichols, K.K., Bierman, P.R., Eppes, M.C., Caffee, M., Finkel, R., Larsen, J., 2005b. Deciphering the Late Pleistocene and Holocene history of the complex Chemehuevi Mountain piedmont using ^{10}Be and ^{26}Al. American Journal of Science 305, 345–368.

Nishiizumi, K., Winterer, E.L., Kohl, C.P., Klein, J., Middleton, R., Lal, D., Arnold, J.R., 1989. Cosmic ray production rates of 10Be and 26Al in quartz from glacially polished rocks. Journal of Geophysical Research 94, 17,907–17,915.

O'Hara, S.L., 1997. Human impacts on dryland geomorphic processes. In: Thomas, D.S.G. (Ed.), Arid Zone Geomorphology: Process, Form and Change in Drylands. John Wiley & Sons Ltd., London, pp. 639–658.

Persico, L.P., Nichols, K.K., Bierman, P.R., 2005. Tracking painted pebbles: short-term rates of sediment movement on four Mojave Desert piedmont surfaces. Water Resources Research 41, 1–15.

Phillips, W.M., McDonald, E.V., Reneau, S.L., Poths, J., 1998. Dating soils and alluvium with cosmogenic ^{21}Ne depth profiles: case studies from the Pajarito Plateau, New Mexico, USA. Earth and Planetary Science Letters 160, 209–223.

Rahn, P.H., 1967. Sheetfloods, streamfloods, and the formation of pediments. Annals of the American Association of Geographers 57, 593–604.

Reheis, M.C., Slate, J.L., Throckmorton, C.K., McGeehin, J.P., Sarna-Wojcicki, A.M., Dengler, L., 1996. Late Quaternary sedimentation on the Leidy Creek fan, Nevada-California: geomorphic responses to climate change. Basin Research 12, 279–299.

Reid, I., Laronne, J.B., 1995. Bed load sediment transport in an ephemeral stream and a comparison with seasonal and perennial counterparts. Water Resources Research 31, 773–781.

Schick, A.P., Lekach, J., Hassan, M.A., 1987. Vertical exchange of coarse bedload in desert streams. In: Frostick, L., Reid, I. (Eds.), Desert Sediments: Ancient and Modern. Geological Society Special Publication, London, pp. 7–16.

Small, E.E., Anderson, R.S., Hancock, G.S., 1999. Estimates of the rate of regolith production using ^{10}Be and ^{26}Al from an alpine hillslope. Geomorphology 27, 131–150.

Stone, J., 2000. Air pressure and cosmogenic isotope production. Journal of Geophysical Research 105, 23753–23759.

Trimble, S.W., 1977. The fallacy of stream equilibrium in contemporary denudation studies. American Journal of Science 277, 876–887.

Wells, S.G., McFadden, L.D., Dohrenwend, J.C., 1987. Influence of Late Quaternary climatic changes on geomorphic and pedogenic processes on a desert piedmont, eastern Mojave Desert, California. Quaternary Research 27, 130–146.

Wells, S.G., McFadden, L.D., Poths, J., 1995. Cosmogenic ^{3}He surface-exposure dating of stone pavements: implications for landscape development. Geology 23, 613–616.

Wells, S.G., Brown, W.J., Enzel, Y., Anderson, R.Y., McFadden, L.D., 2003. Late Quaternary geology and paleohydrology of pluvial lake Mojave, southern California. In: Enzel, Y., Wells, S.G., Lancaster, N. (Eds.), Paleoenvironments and Paleohydrology of the Mojave and Southern Great Basin Deserts. Geological Society of America, Boulder, CO, pp. 79–114.